

1 **Back to basic, optical evaluation of motion in electric fields for specific surface**
2 **charge determinations**

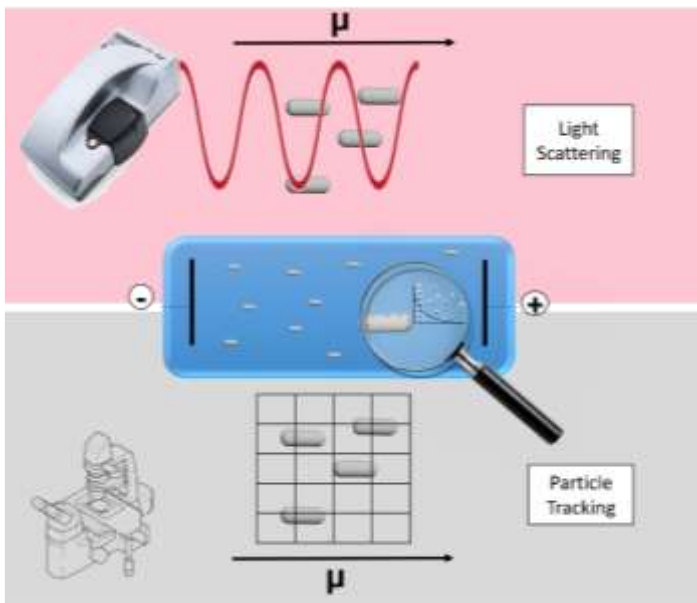
3 Julio Bastos-Arrieta, LinLin Wang, Aidee Garcia-Zintzun, and Juliane Simmchen*

4 Physical Chemistry TU Dresden, Zellescher Weg 19, 01062 Dresden, Germany

5 *Corresponding Author: juliane.simmchen@tu-dresden.de

6

7 TOC:



8

9

10

11 **ABSTRACT**

12 Dynamic Light Scattering (DLS) is a widely used tool for the measurement of Zeta Potential,
13 taking benefit of automated detection to achieve fast measurements. However, the
14 mathematical criteria on which the calculations in DLS devices are based, imply a very narrow
15 set of conditions. One of them is a perfect spherical shape, since a hard sphere model is
16 assumed for calculating scattering patterns and therefore the analysis of different shapes could
17 result in significant deviations. One frequent example where the determination of the surface
18 charge in rod-shaped colloids is required, is the characterization of bacterial surface charge,
19 which is complicated by complex surface properties. To test whether the commercial device
20 gives a reasonable approximation, we constructed a homemade optical device and tested
21 inorganic spherical and rod-shaped SiO_2 particles and compared them to a model bacterium.
22 A different case is the determination of surface potentials of light sensitive materials under
23 illumination. Commercial devices often do not allow the additional implementation of light
24 sources other than the laser, but our setup flexibly enables us to plug in different illuminations.

25

26 **KEYWORDS**

29 Introduction

30 Colloidal science has evolved in a plentitude of ways over the last century, starting from
31 synthetic strategies such as the Stöber synthesis,^[1] hot injection^[2] or the polyol synthesis,^[3] to
32 the advances in instrumentation and characterization techniques like electron microscopy,
33 spectroscopy or light scattering. Significant concepts to understand the properties of charged
34 colloidal surfaces were developed since the nineteenth century.^[4] H.v.Helmholtz himself
35 introduced the idea of an electrical double layer (EDL). EDL refers to the ionic environment
36 surrounding a charged colloidal particle, which consists of hydrated and bare ions of mostly
37 opposite charge, neutralizing the charged groups on the colloid's surface. In the 1930's, this
38 concept was refined by L.G.Gouy and D.L.Chapman, including the concept of a diffuse double
39 layer around the particle, as well as the influence of steric effects.

40 The EDL consists firstly of a layer where bare ions (Stern layer), followed by a layer of hydrated
41 ions, are strongly bounded to the colloid surface. Beyond this layer, the diffuse layer is found.
42 There, the hydrated ions are less firmly associated to the colloid and the ion concentrations
43 depart from the electroneutrality values.^[5,6] The diffuse layer depends on factors as the pH and
44 ionic strength; it is formed by ions with the same and opposite charge of the colloid's surface.^[7]

45 The EDL is a dynamic construct and therefore does not lead the colloid to have zero net
46 charge, which becomes obvious when an electric field is applied to the colloidal suspension.
47 The colloids then move towards the electrode with opposite charge; i.e. electrophoresis.^[7,8]
48 Thus, within the diffuse layer a hypothetical shear/slipping plane or boundary exists, inside of
49 which the ions move in the same direction as the charged colloid; meanwhile the ions outside
50 this boundary zone migrate as the dispersing fluid.^[5] These interactions lead to the presence
51 of an electrokinetic potential in the shear plane, known as Zeta Potential (ζ).

52 Due to this definition, Zeta Potentials are difficult to measure directly but can be calculated by
53 the evaluation of the electrophoretic mobility (μ) of particles in an electric field. According to
54 the Henry Equation

$$55 \mu_e = \frac{2\varepsilon\zeta f_{(k\alpha)}}{3\eta} \quad (1)$$

56 the electrophoretic mobility depends on the viscosity η of the dispersion media (in cP), ε the
57 dielectric constant and the Henry's function $f_{(k\alpha)}$, a parameter depending on the ratio of the
58 particle radius to the thickness of the EDL. Here, it becomes obvious that the shape of the
59 colloid is of pivotal importance, for example, the frequently used Helmholtz-Smoluchowski
60 approximation gives $f_{(k\alpha)}$ a value of 1.5; considering a double layer which is thin compared
61 with the particle radius with a spherical geometry^[9] (Equation 2)

$$62 \mu_e = \frac{\varepsilon\zeta}{\eta} \quad (2)$$

63 Since the Zeta Potential is used as indicator of the stability of a colloidal system^[10,11] there
64 was a great interest in the development of electrophoresis based techniques with optical
65 evaluation (Particle electrophoresis, Zetameter setup).^[12,13] With the introduction of an
66 automated detection based on laser scattering methods (Dynamic Light scattering, DLS)^[14] the
67 evaluation of Zeta Potentials became frequently used as screening method of production
68 processes. More recently, commercial devices were also improved to allow measurements on
69 biological molecules with low scattering intensities and therefore, moved into the focus of

70 biologists.^[15–17] Lately, the interest in characterizing the surface of bacteria as biological
71 colloids has grown due to different applications in biofilms,^[18–20] biotechnological advances^[21]
72 and biohybrid micromotors.^[22,23]

73 Given this interest, microbiologists evaluate the charge of bacteria by a qualitative method
74 based on electrostatic interactions of the bacterial surface with strongly charged fluorescent
75 biomolecules. Thus, alterations in the overall charge of the cell (environmentally induced or
76 due to mutations) can be screened by analyzing the capability to bind negatively or positively
77 charged proteins.^[24] Despite the unknown nature of interaction, this method gives reasonable
78 insights as long as all other factors are kept constant. This limit makes evident the need of
79 other strategies for bacteria surface characterization. Most of these characterization
80 techniques are based on the electrophoretic/electrostatic features of bacteria:
81 microelectrophoresis, electrostatic interaction chromatography, aqueous two phase
82 partitioning, isoelectric equilibrium analysis, and among others, electrophoretic DLS.^[13]

83 The general aim of this study is to determine how different conditions and shapes affect the
84 electrophoretic mobility of colloids using a Zetameter setup; and compare the obtained values
85 with the widely used DLS method. To do so, we construct a home-made electrophoresis setup
86 (Zetameter), in which the calculations of electrophoretic mobility are based on direct
87 observation of particles moving under an applied electric field. The analysis of different
88 particles by both methods, evidenced agreement among the Zeta Potential values obtained
89 for spherical silica particles; but significant differences were found for the values rod-shaped
90 silica particles. These findings are compared to the equivalent results of bacteria as rod-
91 shaped living particles with different physicochemical properties. Thus, we used the Zetameter
92 to calculate the electrophoretic mobility of a *Lactobacillus* strain used for the preparation of
93 “Sauerkraut”; as an alternative methodology; considering that the deviation from the typical
94 spherical shape could result in laser scattering effects in DLS measurements. In addition, we
95 show the feasible application of our Zetameter setup to analyze particles with light induced
96 activity, like spherical TiO₂, particles, as an example of direct observation of light induced
97 phenomena, which is not possible in the DLS approach.

98

99 **Results and Discussion**

100 There are plenty of aspects to compare both methods, obvious are the ease of use, the cost
101 of equipment, training necessity, adaptability of the method among others. Due to single use
102 cells, DLS has clear advantage over the Zetameter in terms of handling the samples.
103 Concerning the analytics, the Zetasizer device uses dynamic light scattering to evaluate the
104 particle speed. For this method, a monochromatic light source (usually a laser) is required.
105 When the laser light hits a small particle, the light is scattered. These scatter patterns are
106 dependent on the size (and shape) of the particle, which is accounted for in the mathematical
107 model. Since the particles are moving, the signals change dynamically and also interact with
108 the scattered light of the surrounding colloids, leading to interference in the signals. The
109 detected signal fluctuations are transformed into an autocorrelation function, which is further
110 processed to extract more user friendly data values. In the Zetameter instead, Particle Tracking
111 Analysis (PTA), is used to obtain particle speed data. In this simple and reliable method, the
112 time resolved trajectories are tracked from videomicroscopy, reducing the system to a two
113 dimensional electrophoretic one, causing the loss of the actual 3D movement of the
114 particles.^[25] Particles analyzed by PTA must have stronger scattering than the background
115 (which is the case of bacteria); leading to a lower density of results than in DLS. While the

116 asymmetric scattering is especially disturbing for increased sizes in the DLS, the problem of
117 the settling down of large particles is critical in both methods. One advantage of the more
118 laborious Zetameter strategy is the feasibility of *in situ* observation of kinetic phenomena as
119 assembly of particles, the analysis of fluorescent particles without costly equipment or the
120 application of special irradiations. However, when in DLS heavy particles are removed from
121 the observation fields by sedimentation, in the Zetameter the osmotic influence in vicinity of
122 the wall can be rarely avoided for particles with a density mismatch.

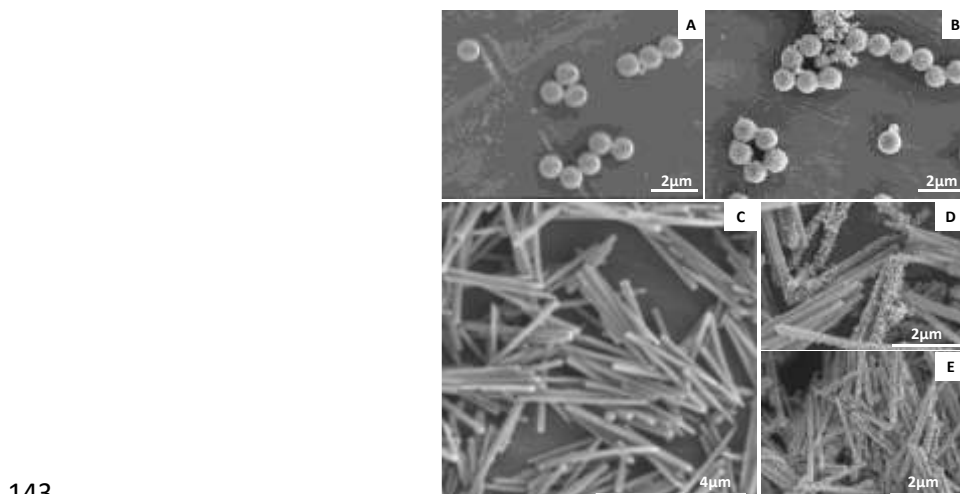
123 The Zeta Potential values are obtained using **Equation 2** in the Zetameter methodology. As
124 previously stated, the suitability of the Helmholtz-Smoluchowski approximation is based on a
125 spherical shape and a thin EDL in comparison with the particle radii.^[5]

126

127 Evaluation of Silica particles

128 Both, SiO₂ spherical and rod-shaped particles were synthesized by previously established
129 procedures.^[26,27] The size and shape of the silica rods were tuned to be comparable to the
130 bacteria (see Figure 1). In the case of raw silica spherical particles, the ζ values obtained by
131 Zetameter and DLS ($-33\pm 4\text{mV}$ and $-34\pm 3\text{mV}$; respectively) are shown in Figure 2A. T-test
132 revealed that they are not statistically different. Nevertheless, the values for rod-shaped
133 particles presented in Figure 2B ($-23\pm 1\text{mV}$ and $-26\pm 3\text{mV}$) show a statistically significant
134 difference when T-test was carried out.

135 In order to demonstrate how surface functionalization can influence the Zeta Potential
136 calculations, Silica particles were functionalized via two different strategies to obtain a
137 coverage of the surface with amino and thiol groups, both binding readily to Au surfaces.
138 Subsequently, we attached or grew gold nanoparticles (Au-NPs) on the surface (see Figure
139 1B, 1D and 1E and Supplementary Information 1, SI1). Thus, we changed not only the
140 chemical and charge properties, but also modified the optical properties of the composites,
141 which influence the scattering patterns and intensities of the laser (Refractive Index (RI) SiO₂:
142 $1.5534^{[28]}$ RI Bacteria: $\sim 1.38^{[29]}$ RI Au: $0.58^{[30]} - 0.88^{[31]}$).



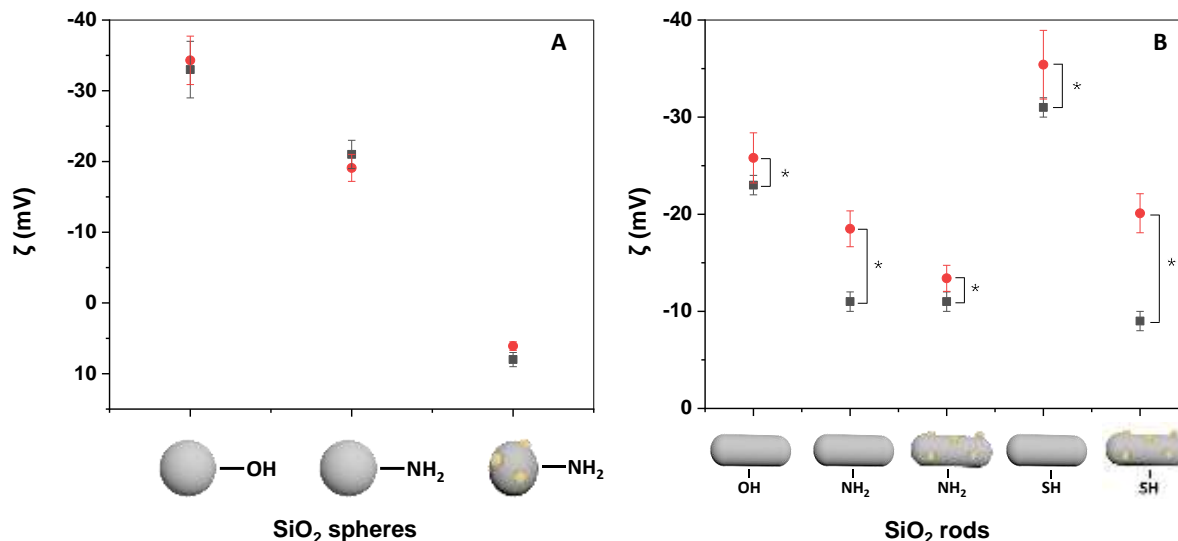
143

144 **Figure 1:** SEM micrographs of A) 1 μm SiO₂ and B) Au@SiO₂-NH₂ spheres. C) SiO₂ rods, D)
145 Au@ SiO₂- NH₂ rods and E) Au@SiO₂-SH rods

146

147 Au-NPs grown on the amine functionalized particles (Au@SiO₂ -NH₂ hard sphere and
148 Au@SiO₂ rods-NH₂, Figure 1B and 1D), are slightly smaller than the ones attached to the

149 thiolated particles (Au@SiO₂-SH), as seen in Figure 1E. This size difference owes to the
 150 different synthetic methods (*in situ* growth versus attachment), but does not affect the study.
 151 In comparison to the plain spheres, the potential values obtained by the determination of
 152 electrophoretic mobility by Zetameter setup and DLS for the Au@SiO₂ particles are not
 153 significantly different (+8±1mV and +6±1mV). The presence of the Au-NPs on the surface of
 154 the silica spheres seems not to produce deviations (see Figure 2A and SI2).
 155 In agreement with the abovementioned results for the plain silica rods, the differences between
 156 the methods are even larger in the case of Au@SiO₂ rods (see Figure 2B and SI2). The most
 157 pronounced difference is seen for Au@SiO₂-SH rods (-9±1mV and -20±2mV). However,
 158 despite the fact that we observed particles with different surface properties, the migration of all
 159 particles seems to be governed mainly by a hydrodynamically favorable orientation (the rod-
 160 shaped particle in line with the flow, see Figure SI5). The shape caused a clear deviation when
 161 comparing the data obtained by Zetameter with the DLS data. T-tests revealed significantly
 162 different values for all analyzed samples. Since the Zeta Potential is an artificial value, we have
 163 no direct way of its determination, but in line with our theoretical assumptions, we find that a
 164 rod-shaped geometry seems to put clear limits to the application of DLS.
 165
 166



167
 168 **Figure 2:** Comparison of the mean Zeta Potential and standard deviations values obtained
 169 using electrophoretic mobility (black squares, at 40V) and dynamic light scattering (red
 170 squares) of SiO₂ spherical (A) and SiO₂ rod particles (B) Statistical different values: * P ≤ 0.05
 171

172 As expected, the DLS and Zetameter results have good agreement for spherical particles. Both
 173 techniques can be used complimentary and the laser scattering gives reliable measurements,
 174 for which the DLS has replaced manual measurements for most laboratory uses. Also
 175 concerning the inorganic rod-shaped particles we confirm the expected deviations, leading to
 176 values that are significantly different for plain, functionalized and Au-composites.

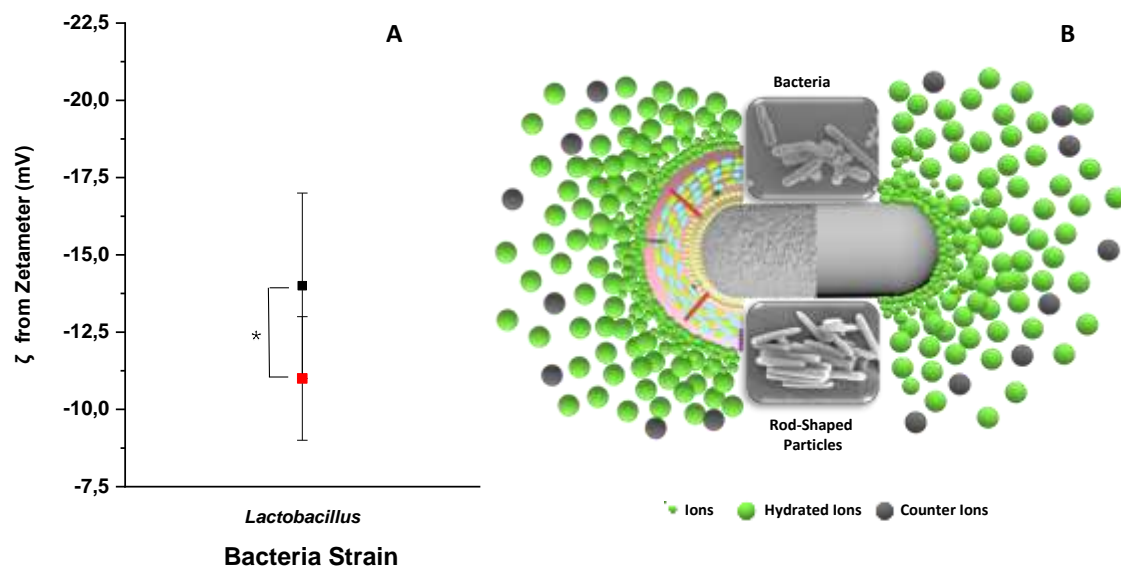
177 Evaluation of Bacterial cells

178 In order *measure and* calculate the Zeta Potential of a real rod-shaped living particle we chose
 179 a type of Lactobacillus, autochthonous to the German culinary culture (see Experimental
 180 Section). This bacterium has a pronounced rod-shaped geometry (see Figure 3), no flagella
 181 that could lead to additional drag effects [37] and it is a non-motile species; so not overlaying
 182 movements are to be expected. T-test showed significant difference in Zeta Potential values

183 of *Lactobacillus* strain, obtained by the Zetameter and DLS methodologies ($-14\pm 3\text{mV}$ and $-11\pm 2\text{mV}$, respectively; see SI3). These deviations can be attributed to its elongated shape and
 184 agree with the abovementioned differences for the rod silica particles. As for silica rods, the
 185 bacteria orientation during the electrophoretic assays is hydrodynamically favorable, i.e. in line
 186 with the flow (see SI5). What apparently does not play an important role is the soft and porous
 187 structure of the Bacterial surface. However, to evaluate the influence on the surface slip and
 188 therefore the hydrodynamics in vicinity of the particles and the electrophoretic mobility, more
 189 controlled modifications of bacterial morphologies and surface properties would be needed.
 190 Also additional shape deviations caused by substructures of the bacterial surface such as pili,
 191 or fimbriae are not considered, even though they are expected to have a rather important
 192 influence on the drag.^[37]

194 Further deviations between the values obtained can be due to the structural differences of the
 195 bacteria wall. In general, cell surfaces are highly dynamic and respond strongly to external
 196 stimuli, by adsorptions of ions and others substances, altering the surface properties.^[33] Even
 197 though the morphology and size of the studied silica rods and *Lactobacillus* are similar (see
 198 SEM insets in figure 3B), the distribution of charged groups on bacterial surfaces may not be
 199 homogeneous,^[34] making the bacterial surface chemically and structurally more complex than
 200 the one inorganic colloidal particles, affecting the EDL interactions (Schematically presented
 201 in Figure 3B).^[35,36]

202



203

204 **Figure 3:** Comparison of the mean Zeta Potential and standard deviations values obtained
 205 using electrophoretic mobility (black squares, at 40V) and dynamic light scattering (red
 206 squares) of *Lactobacillus* (A) and schematic representation of the differences of the EDL
 207 between bacteria and rod particles (B). Statistical different values: * $P \leq 0.05$

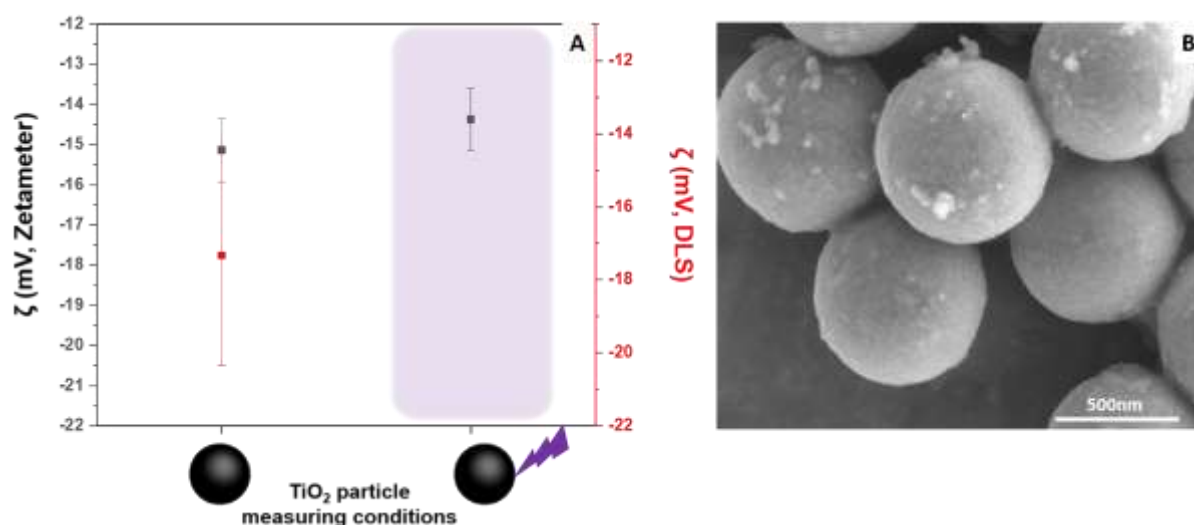
208

209 These biologically specific restrictions combined with the limitations of DLS for the
 210 measurement of complex shapes; show the importance of the comparison of both strategies,
 211 to evaluate their suitability for the analysis of bacteria surface. Despite the calculated
 212 statistically significant deviations between both methods, the obtained absolute and relative
 213 differences between the DLS and the Zetameter results are small and for most biological
 214 applications probably not of major importance.

215

216 Evaluation of the influence of illumination on the electrophoretic mobility of photoactive
217 particles

218 One of the major drawbacks of automated DLS devices is the relative lack of flexibility of in
219 terms of added experimental conditions. In order to evaluate the surface properties of active
220 photocatalytic or photoswitchable materials, *in situ* illumination is required, which is not
221 implementable in most commercial devices. Here, our setup connected to an optical
222 microscope is an excellent way to evaluate the changes that these particles undergo. To
223 evaluate these changes, we chose simple spherical TiO₂ particles of a mixed phase rutile
224 anatase, which have shown a low photoinduced activity in water.^[37]



225

226 **Figure 4:** Evaluation of the mean Zeta Potential and standard deviations values obtained using
227 DLS in red squares and the Zetameter setup at 40V in black squares (A) and SEM image of
228 the titania particles (B)

229 In Figure 4 we see the different values obtained for titania particles in water (check SI4 for
230 values). The deviation for non UV illuminated particles is rather large considering their perfect
231 spherical shape, which could be due to the influence of the laser, or alternatively, due to the
232 small part of UV light present in the microscope illumination.

233 UV light in water seems to decrease the potential slightly, but no pronounced effect can be
234 observed, which is coherent with the low activity we found for these particles. However, the
235 method gave access to an interesting data point, that we could not obtain using a commercial
236 DLS setup. Further interesting data is expected by using different media (e.g. H₂O₂) as well as
237 other, maybe switchable particles.

238

239 Conclusions

240 We evaluated the suitability of two different methodologies (DLS and Zetameter) for the
241 determination of Zeta Potential values of different shapes of colloids. The comparison between
242 the values calculated from both strategies resulted similar values in the case of spherical silica
243 particles. On the contrary, all analyzed rod-shaped particles showed the expected deviations
244 in the DLS measurements due to their distinct rod shapes. In case of bacterial cell, the

245 deviations from spherical shape impact the DLS values, but the deviations are rather small, so
246 that the values can give a reasonable approximation. However, no information about the
247 surface morphology can be obtained, despite the fact that it would affect directly the
248 hydrodynamics and the electrophoretic motion. Since it would be present in DLS as well as the
249 Zetameter, no conclusions can be drawn. On the other side, this regained method can become
250 a powerful tool evaluating colloids under different illumination conditions, as was proven by the
251 evaluation of the titania particles.

252

253 **Experimental Section**

254 Materials and reagents:

255 Tetraethoxysilane (TEOS), (3-Aminopropyl) triethoxysilane (APTES), Ammonia (NH₃, aq.
256 25%), Gold (III) chloride trihydrate (HAuCl₄·3H₂O), 1-Pentanol, 3-
257 Mercaptopropyltrimethoxysilane (MPTMS), sodium citrate, trisodium citrate,
258 Polyvinylpyrrolidone (PVP; Molar weight: 40K) were purchased from Sigma Aldrich, of
259 analytical grade and used as received without further treatment. Ethanol (EtOH, absolute) was
260 purchased from VWR and potassium chloride from J.T. Baker. Titanium (IV) iso-propoxide
261 (TTIP) was purchased from Alfa Aesar Co. Ltd. Dodecylamine (DDA) was obtained from Fluka.
262 Milli-Q water was used for preparing aqueous solutions

263 Preparation and functionalization of 1 μm SiO₂ spherical particles:

264 1.9 ml TEOS were diluted in 13 ml isopropanol and mixed with 0.7 ml NH₃ (25%) in 1.4 ml H₂O.
265 The solution was stirred at room temperature and aged for 60 min at 50°C to obtain seeds. A
266 solution of 7 ml TEOS in 300 ml propanol was added to the seed solution under constant
267 stirring. Subsequently 20 ml NH₃ (25%) in 40 ml of water were added and heated to 50°C. As
268 last step 120 ml TEOS were added at an addition rate of 0.5 g/min. Several filtration and
269 washing steps with water are required to remove NH₃ and solvent residues.

270

271 Preparation and functionalization of SiO₂ rods:

272 As described somewhere else,^[26] the preparation of 2-3μm SiO₂ rods requires a solution of 1g
273 of PVP in 10 ml of 1-pentanol. Then, 1 ml of ethanol, 340μl of water and 80μl of sodium citrate
274 (0.18 M) were added and stirred for 5min. Then, 200μl of ammonia and 60μl of TEOS were
275 added. The solution was stirred for 5 min. and then left under static conditions for 18h. The
276 obtained rods were washed several times with ethanol and separated by centrifugation.

277

278 Amine (-NH₂) or thiol (-SH) Functionalization of SiO₂ spheres or rods:

279 100 mg of SiO₂ particles or rods were dispersed in 5mL of EtOH; then 150μl of APTES (for
280 amine functionalization) or 150μl of MPTMS (for thiol functionalization) and 300μl of ammonia
281 were added. The particle suspension were stirred overnight. The washing procedure included
282 centrifugation and rinse several times with ethanol.

283 Amine groups (-NH₂) have partial positive charge, making that APTES functionalized particles
284 have less negative surface charge as shown in SI2 Table I. Thus, the synthesis of Au NPs with
285 the syringe pump approach is driven firstly by the immobilization of the Au NPs precursor
286 (AuCl₄⁻) and then the reducing stage with the ascorbic acid and trisodium citrate. The process
287 is favored due to the known affinity of gold nanoparticles to amine moieties.^[38]

288 Thiol groups (-SH) maintain the overall negative charge of the raw particles.^[38,39] Chemical
289 affinity of Au with thiol moieties leads to the attachment of previously synthesized particles to

290 thiolated surfaces.^[38,39] Moreover, it is favored due to the positive ζ of the Au NPs as shown in
291 SI 2 Table I.

292

293 Preparation of Au@amine functionalized SiO₂ particles or rods.

294 A seed growth approach to obtain uniform gold nanoparticles was adapted as follows.^[40] In a
295 three necked flask, containing a suspension 25mg of the SiO₂ particles or rods in 20ml of water
296 was stirred vigorously. Simultaneously, two solutions: A (8 ml H [AuCl₄⁻] (1%) + 2 ml water)
297 and B (2 ml ascorbic acid (1%) + 1 ml trisodium citrate (1%) + 7 ml water) were drop-wise with
298 syringe pump at a rate of 20ml·h⁻¹. The resulting suspension was boiled for 30min; and the
299 particles were separated by centrifugation and washed several times with water.

300

301 Preparation of Au@thiol functionalized SiO₂ rods:

302 The preparation of Au was adapted from somewhere else.^[41] 10ml of tetralin, 10ml of
303 Oleylamine(OAm) and 0.1g of HAuCl₄·3H₂O were combined and magnetically stirred under N₂
304 flow for 10 min. Then, a solution 0.5 mmol of Tetrabutylammonium bromide (TBAB), 1ml of
305 tetralin and 1mL of OAm (mixed by sonication) were injected into the abovementioned solution.
306 The mixture changed to a deep purple and left to react for 1h. The nanoparticles were
307 precipitated by adding 60ml of ethanol, and then washed with ethanol and separated by
308 centrifugation. These Au NPs (with a Zeta Potential value of +31mV) were dispersed in 5ml of
309 chloroform. 25mg of the thiolated SiO₂ rods were suspended in 3ml of ethanol. Then, 3ml of
310 suspension of gold nanoparticles in chloroform were added. The mixture was shaken overnight
311 and separated by centrifugation followed by washing steps with ethanol.

312 Preparation of TiO₂ particles

313 The synthesis is based on the hydrolysis and condensation reaction of TTIP^[42,43]: 0.18 ml of
314 water was added to mixture solution containing 105 ml of methanol and 45 ml of acetonitrile.
315 Then 0.28 g of DDA was dissolved in the mixture under stirring. After stirring for 10 min, 1 ml
316 of TTIP was added drop wisely and stirred for 12 h. DDA acted as a catalyst and molecular
317 template to introduce the pores into the TiO₂ particles. Then the particles were washed with
318 methanol three times and dried at 80°C. The particles were heated in tubular furnace under
319 nitrogen flow for 2h at 600°C.

320 Preparation of *Lactobacillus*

321 Autochthonous *Lactobacillus* from cabbage (*Brassica oleracea*) was cultivated by a traditional
322 recipe: the cabbage was sliced into thin stripes, about 5 wt% of salt were added and the mixture
323 was pounded until liquid emerged from the vegetable and covered the mixture. Then the
324 mixture was covered with leafs and left fermenting at about 27°C for seven days. After that,
325 the mixture was transferred to a cool place and left maturing for several weeks prior to use.
326 Before characterization, the bacteria were centrifuged, washed and prepared for the individual
327 characterization steps.

328

329 Electron Microscopy Characterization

330 Scanning electron microscopy (SEM) was performed on Aluminum covered holders in a Zeiss
331 DSM 982 Gemini instrument. Bacteria samples were washed three times and collected after
332 centrifugation at 3000rpm, and resuspended in 3% glutaraldehyde solution. Then, silicon
333 wafers were incubated with bacteria suspension for 30min. Afterwards, bacteria were
334 dehydrated in a series of increasing aqueous ethanol concentrations (30%, 50%, 60%, 75%,
335 90% and 100%) for 5 min in each solution. The same procedure was repeated for the same

336 concentrations and times for Hexamethyldisilazane solutions. The samples were then dried
337 overnight.

338

339 Determination of Zeta Potential by means of DLS

340 A Malvern Zetasizer® Nano ZSP with a10mW red laser (632.8 nm) was used to record the
341 Zeta Potential of the different type of silica particles and bacteria. In each case, the sample
342 was equilibrated for 1 min at 25 °C before starting the measurements. Three measurements,
343 each consisting of 30 runs were performed for each sample.

344

345 Determination of Zeta Potential by means of electrophoretic mobility via a Zetameter set-up:

346 An electrophoretic cell was filled with the particle suspension to be studied. Thus, two Pt mesh
347 electrodes plugged to a power source, were immersed in the dispersion and then; increasing
348 voltages (from 10V to 50V) were applied. To avoid bubble formation on the electrodes, their
349 polarity were changed and then decreasing voltages (from 50V to 10V) were applied.
350 Conductivity was kept to $1,411 \times 10^{-3} \text{ S}\cdot\text{cm}^{-1}$ value using KCl 0.01M for inorganic particles and
351 with the appropriate dilutions of the bacteria suspensions. Electrophoretic mobility of bacteria
352 was carried out analyzing at least 90 bacteria cell per voltage. An analogue procedure was
353 used for the inorganic counterparts. The electrophoretic movement of the particles were
354 recorded with an Inversed Optical microscope (Carl Zeiss Microscopy GmbH Germany)
355 equipped with a Zeiss Colibri lamp; using an acquisition time of 40ms and a 50x long working
356 distance objective (Zeiss® LD EC Epiplan-NEOFLUAR 50x/0.55 DIC 60). The analysis of the
357 recorded videos was carried out using tracking tool from ImageJ software version 1.52i
358 (National Institute of Health, USA)^[44]

359 T-test: statistically significant differences in mean ζ for all SiO₂ rods and *Lactobacillus* with 95%
360 confidence interval.

361

362 **References:**

- 363 [1] W. Stöber, A. Fink, E. Bohn, *J. Colloid Interface Sci.* **1968**, 26, 62.
364 [2] C. B. Murray, D. J. Norris, M. G. Bawendi, *J. Am. Chem. Soc.* **1993**, 115, 8706.
365 [3] F. Fievet, J. P. Lagier, B. Blin, B. Beaudoin, M. Figlarz, *Solid State Ionics* **1989**, 32–33,
366 198.
367 [4] D. Myers, *Surfaces, Interfaces, and Colloids: Principles and Applications*, **1991**.
368 [5] G. V. Lowry, R. J. Hill, S. Harper, A. F. Rawle, C. O. Hendren, F. Klaessig, U.
369 Nobbmann, P. Sayre, J. Rumble, *Environ. Sci. Nano* **2016**, 3, 953.
370 [6] R. E. G. Van Hal, J. C. T. Eijkel, P. Bergveld, *Adv. Colloid Interface Sci.* **1996**, 69, 31.
371 [7] S. Bhattacharjee, *J. Control. Release* **2016**, 235, 337.
372 [8] H. Morgan, N. G. Green, *AC Electrokinetics*, **2003**.
373 [9] R. H. Ottewill, R. L. Rowell, *Zeta Potential in Colloids Sciences Principles and*
374 *Applications*, **1989**.
375 [10] P. P. Esteban, A. T. A. Jenkins, T. C. Arnot, *Colloids Surfaces B Biointerfaces* **2016**,
376 139, 87.
377 [11] K. Makino, H. Ohshima, *Langmuir* **2010**, 26, 18016.
378 [12] M. Rosoff, *Nano-Surface Chemistry Edited By*, **2001**.

- 379 [13] W. W. Wilson, M. M. Wade, S. C. Holman, F. R. Champlin, *J. Microbiol. Methods*
380 **2001**, *43*, 153.
- 381 [14] P. A. Hassan, S. Rana, G. Verma, *Langmuir* **2015**, *31*, 3.
- 382 [15] A. P. Minton, *Anal. Biochem.* **2016**, *501*, 4.
- 383 [16] R. E. Martinez, O. S. Pokrovsky, J. Schott, E. H. Oelkers, *J. Colloid Interface Sci.*
384 **2008**, *323*, 317.
- 385 [17] S. Halder, K. K. Yadav, R. Sarkar, S. Mukherjee, P. Saha, S. Haldar, S. Karmakar, T.
386 Sen, *Springerplus* **2015**, *4*, 1.
- 387 [18] G. Roeselers, M. C. M. Van Loosdrecht, G. Muyzer, *J. Appl. Phycol.* **2008**, *20*, 227.
- 388 [19] J. L. Shore, W. S. M'Coy, C. K. Gunsch, M. A. Deshusses, *Bioresour. Technol.* **2012**,
389 *112*, 51.
- 390 [20] S. G. Hays, W. G. Patrick, M. Ziesack, N. Oxman, P. A. Silver, *Curr. Opin. Biotechnol.*
391 **2015**, *36*, 40.
- 392 [21] S. Sarria, N. S. Kruyer, P. Peralta-Yahya, *Nat. Biotechnol.* **2017**, *35*, 1158.
- 393 [22] J. Bastos-Arrieta, A. Revilla-Guarinos, W. E. Uspal, J. Simmchen, *Front. Robot. AI*
394 **2018**, *5*, 97.
- 395 [23] M. M. Stanton, J. Simmchen, X. Ma, A. Miguel-López, S. Sánchez, *Adv. Mater.*
396 *Interfaces* **2016**, *3*, DOI 10.1002/admi.201500505.
- 397 [24] A. Peschel, M. Otto, R. Jack, *J. Biol. ...* **1999**, *274*, 8405.
- 398 [25] A. Malloy, B. Carr, *Part. Part. Syst. Charact.* **2006**, *23*, 197.
- 399 [26] A. Kuijk, A. Van Blaaderen, A. Imhof, *J. Am. Chem. Soc.* **2011**, *133*, 2346.
- 400 [27] M. Bele, O. Siiman, E. Matijević, *J. Colloid Interface Sci.* **2002**, *254*, 274.
- 401 [28] G. Ghosh, *Opt. Commun.* **1999**, *163*, 95.
- 402 [29] A. E. Balaev, K. N. Dvoretzki, V. A. Doubrovski, *Saratov Fall Meet. 2002 Opt. Technol.*
403 *Biophys. Med. IV* **2003**, *5068*, 375.
- 404 [30] L. Gao, F. Lemarchand, M. Lequime, *Thin Solid Films* **2011**, *520*, 501.
- 405 [31] A. You, M. A. Y. Be, I. In, **2017**, *095024*, DOI 10.1063/1.5004727.
- 406 [32] M. Potomkin, V. Gyrya, I. Aranson, L. Berlyand, *Phys. Rev. E* **2013**, *87*, 53005.
- 407 [33] ... Magdanz, Veronika, *Adv. Biosyst.* **n.d.**
- 408 [34] S. Stankowski, *Biophys. J.* **1991**, *60*, 341.
- 409 [35] A. T. Poortinga, A. Thijs, *Electric Double Layer Interactions in Bacterial Adhesion and*
410 *Detachment*, **2001**.
- 411 [36] E. Kłodzińska, M. Szumski, E. Dziubakiewicz, K. Hryniewicz, E. Skwarek, W. Janusz,
412 B. Buszewski, *Electrophoresis* **2010**, *31*, 1590.
- 413 [37] L. Wang, M. N. Popescu, F. Stavale, A. Ali, T. Gemming, J. Simmchen, *Soft Matter*
414 **2018**, *14*, 6969.
- 415 [38] D. A. Giljohann, D. S. Seferos, W. L. Daniel, M. D. Massich, P. C. Patel, C. A. Mirkin,
416 *Angew. Chemie Int. Ed.* **2010**, *49*, 3280.
- 417 [39] F. Frederix, K. Bonroy, W. Laureyn, G. Reekmans, A. Campitelli, W. Dehaen, G.

- 418 Maes, *Langmuir* **2003**, *19*, 4351.
- 419 [40] C. Ziegler, A. Eychmüller, *J. Phys. Chem. C* **2011**, *115*, 4502.
- 420 [41] S. Peng, Y. Lee, C. Wang, H. Yin, S. Dai, S. Sun, *Nano Res.* **2008**, *1*, 229.
- 421 [42] S. Tanaka, D. Nogami, N. Tsuda, Y. Miyake, *J. Colloid Interface Sci.* **2009**, *334*, 188.
- 422 [43] L. Wang, M. N. Popescu, F. Stavale, A. Ali, T. Gemming, J. Simmchen, *Soft Matter*
423 **2018**, *14*, 6969.
- 424 [44] J. Schindelin, I. Arganda-Carreras, E. Frise, V. Kaynig, M. Longair, T. Pietzsch, S.
425 Preibisch, C. Rueden, S. Saalfeld, B. Schmid, *Nat. Methods* **2012**, *9*, 676.

426

427 **Acknowledgements**

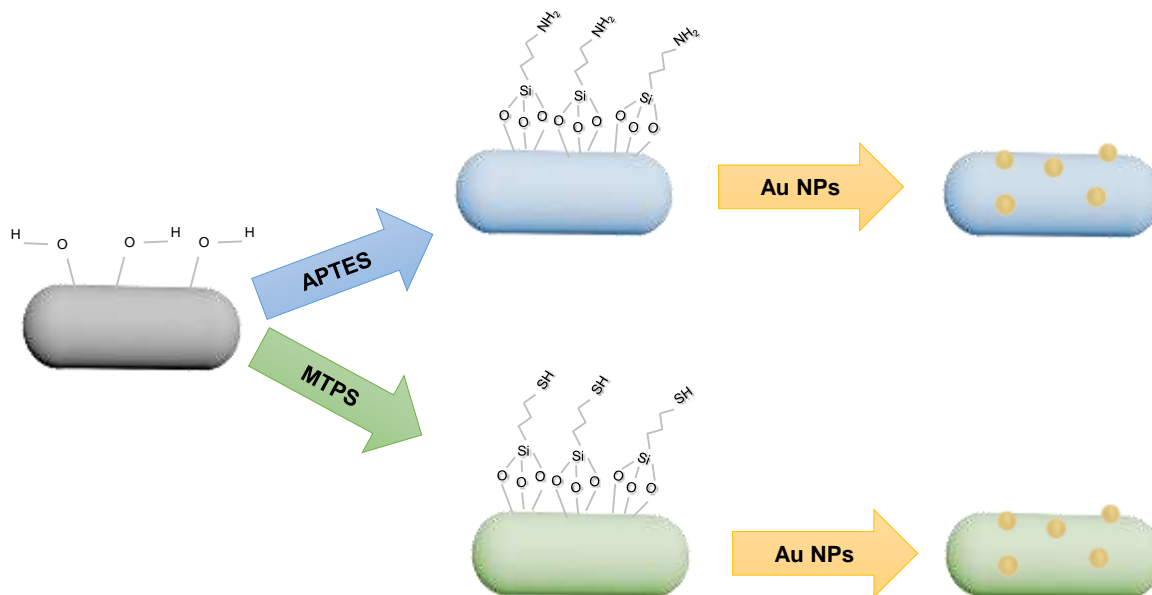
428 The authors thank the SMWK Saxony for the TG70 grant BACMOT (100315856) and J.S.
429 thanks the Volkswagen foundation for the Freigeist fellowship (grant number 91619). LL.W.
430 would like to acknowledge the China Scholarship Council (CSC) for the financial support. All
431 authors acknowledge Dr. M.N.Popescu for critical readings and suggestions and Dr. A. Revilla
432 for initial discussions on mutant bacteria.

433

434

435 **Supplementary Information (SI)**

436 **SI 1:** Schematic summary of the chemical functionalization of silica rods.



437

438 **SI 2: Table I:** Summary results for the determination of Zeta Potential of SiO₂ sphere and rod
 439 particles by the two studied approaches. T-test: non-statistically significant differences with
 440 95% confidence interval in mean ζ for spherical particles. Statistical different values for mean
 441 ζ of silica rods.

442

| Particle type | ζ from Zetameter (mV) | ζ from Zetasizer (mV) |
|--|-----------------------------|-----------------------------|
| SiO ₂ hard sphere | -33±4 | -34±3 |
| SiO ₂ -NH ₂ hard sphere | -21±2 | -19±2 |
| Au@SiO ₂ -NH ₂ hard sphere | +8±1 | 6±1 |
| SiO ₂ rods | -23±1 | -26±3 |
| SiO ₂ rods-NH ₂ | -11±1 | -19±2 |
| Au@SiO ₂ rods- NH ₂ | -11±1 | -13±2 |
| SiO ₂ rods-SH | -31±1 | -35±4 |
| Au@SiO ₂ rods-SH | -9±1 | -20±2 |
| Au NPs | - | +31±2 |

443

444
445
446
447

SI 3: Table 2: Summary results for the determination of Zeta Potential of *Lactobacillus plantarum* by the studied approaches.

| Sample | ζ from Zetameter (mV) | ζ from Zetasizer (mV) |
|----------------------|-----------------------------|-----------------------------|
| <i>Lactobacillus</i> | -14 \pm 3 | -11 \pm 2 |

448

449

SI 4: Table 3: Summary results for the determination of Zeta Potential of *Lactobacillus plantarum* by the studied approaches.

451
452

| Sample | ζ from Zetameter (mV) | ζ from Zetasizer (mV) |
|---------------------------------|-----------------------------|-----------------------------|
| TiO ₂ particles | -15.1 \pm 0.8 | -17.3 \pm 3 |
| TiO ₂ particles + UV | -14.4 \pm 0.8 | - |

453

454

455

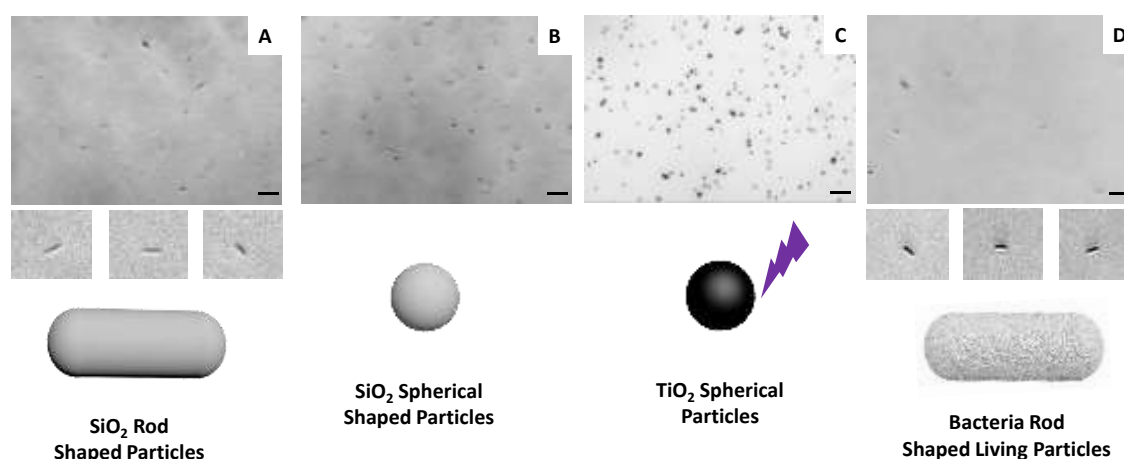
456

457

SI 5: Screenshots of the particle tracking for the determination of the electrophoretic mobility of different rod and spherical SiO₂ particles (A,B), TiO₂ particles under UV-light (C) and bacteria (D) using a Zetameter set-up, with the corresponding inset for the type of motion that rod particles have through the application of the electric field. As it can be seen, inorganic and living rod particle present similar orientation; mostly aligned to the flow, with short fluctuations.

461
462
463
464

465



466